EPJ manuscript No.
(will be inserted by the editor)

arXiv:hep-ph/0608003v1 1 Aug 2006

Gluon shadowing in the Glauber-Gribov model

K. Tywoniuk[1], I. C. Arsene[1], L. Bravina[1,2], A. B. Kaidalov[3], and E. Zabrodin[1,2]

[1] Department of Physics, University of Oslo
0316 Oslo, Norway
[2] Institute of Nuclear Physics, Moscow State University
RU-119899 Moscow, Russia
[3] Institute of Theoretical and Experimental Physics
RU-117259 Moscow, Russia

Received: date / Revised version: date

Abstract. New data from HERA experiment on (diffractive) deep inelastic scattering has been used to parameterize nucleon and Pomeron structure functions. Within the Gribov theory, the parameterizations were employed to calculate gluon shadowing for various heavy ions and compared our results with predictions from other models. Calculations for d+Au collisions at forward rapidities at ultra-relativistic energies have been made and are compared to RHIC data on the nuclear modification factor. Results for gluon shadowing are also confronted with recent data on the nuclear modification factor at $\sqrt{s} = 17.3$ GeV at various values of the Feynman variable x_F, and the energy dependence of the effect is discussed.

PACS. 12.40.Nn Regge theory, duality, absorptive/optical models – 13.60.Hb Total and inclusive cross sections (including deep inelastic processes) – 13.85.-t Hadron-induced high- and super-high-energy interactions (energy > 10 GeV) – 25.75.-q Relativistic heavy-ion collisions

1 Introduction

The fact that the nuclear structure function, F_2^A, per number of constituent nucleons is smaller than the structure function of a single nucleon, F_2^N, for $x < 0.1$ [1] is one of the most intriguing effects in modern high-energy nuclear physics. This effect is called nuclear shadowing. We define the nuclear ratio

$$R\left(\frac{A}{N}\right) \;=\; \frac{F_2^A(x,Q^2)}{A\,F_2^N(x,Q^2)} \qquad (1)$$

which is smaller than unity in the shadowing region. The nuclear ratio has been measured for many nuclei and reveals also an interesting structure for $x > 0.1$ (see [1] for further references). In high-energy hadron-nucleus collisions we probe the partonic structure of the nucleus at low values of x. For a given energy the smallest available values of x of the partons in the nucleus are to be found in the fragmentation region, where $x_F = p_z/p_z^{max}$ of the observed particle is close to 1, which corresponds to large pseudorapidity η.

An understanding of the so-called cold nuclear effects, or initial state effects, in hadron-nucleus collisions are therefore an important benchmark for nucleus-nucleus collisions.

A significant change in the underlying dynamics of a hadron-nucleus collision takes place with growing energy of the incoming particles. At low energies, the total cross section is well described within the probabilistic Glauber model [2], which only takes into account elastic rescatterings of the initial hadron on the various nucleons of the nucleus. Elastic scattering is described by Pomeron exchange. At higher energies, $E > E_{crit} \sim m_N \mu R_A$ corresponding to a coherence length

$$l_C \;=\; \frac{1}{2\,m_N\,x}\,, \qquad (2)$$

the typical hadronic fluctuation length can become of the order of, or even bigger than, the nuclear radius, R_A, and there will be coherent interaction of constituents of the hadron with several nucleons of the nucleus. The sum of all diagrams was calculated by Gribov [3]. In this framework, the diffractive intermediate states has to be accounted for in the sum over subsequent rescatterings. The space-time picture analogy to the Glauber series is lost, as the interactions with different nucleons of the nucleus happens instantaneously. The phenomenon of coherent multiple scattering is referred to as shadowing corrections.

An additional effect which comes into play at high energies, is the possibility of interactions between soft partons of the different nucleons in the nucleus. In the Glauber-Gribov model this corresponds to multi-Pomeron interactions. These diagrams are called enhanced diagrams

Correspondence to: konrad.tywoniuk@fys.uio.no

[1] In the infinite momentum frame, x is the longitudinal momentum fraction of a parton in the nucleon

[4], and can also be understood as interactions between strings formed in the collision. E.g. the triple-Pomeron vertex is proportional to $A^{1/3}$ in hA collisions, and so it becomes very important for collisions on very heavy nuclei.

In what follows we will describe a model for hadron-nucleus collisions in Section 2. In Section 3 we will discuss the experimental data on both inclusive and diffractive deep inelastic scattering (DIS) cross-sections measured at HERA used as input to the model. In Section 4 we will present the results for the shadowing ratio, and also compare them to recent experiments at the Relativistic Heavy Ion Collider (RHIC) in Section 5. In Section 6 we compare our calculations to recent measurements done at much lower energies, $\sqrt{s} = 17.3$ GeV, and discuss the energy dependence of the shadowing effect. We summarize and conclude in Section 7.

2 The Model

We will assume that the nucleus consists of A independent nucleons, in the spirit of the Glauber model. The scattering amplitude of an incoming hadron on a nuclear target, can be expanded in a multiple scattering series [5]

$$\sigma_A \;=\; A\sigma_N \,+\, \sigma_A^{(2)} \,+\, \dots\,, \tag{3}$$

where the first term is simply the Glauber elastic rescattering (see Fig. 1). The second term in (3) is related to diffractive DIS through the AGK cutting rules [6]. It is given by [7]

$$\sigma_A^{(2)} \;=\; -4\pi\, A(A-1) \int \mathrm{d}^2b\, T_A^2(b) \times \int_{M_{min}^2}^{M_{max}^2} \mathrm{d}M^2 \left[\frac{\mathrm{d}\sigma_{hN}^{\mathcal{D}}}{\mathrm{d}M^2\mathrm{d}t}\right]_{t=0} F_A^2(t_{min})\,, \tag{4}$$

where M^2 is the mass of the diffractively produced intermediate state, $T_A(b)$ is the normalized nuclear thickness function and $\mathrm{d}\sigma_{hN}^{\mathcal{D}}/\mathrm{d}M^2\mathrm{d}t$ is the differential cross section for diffractive dissociation of the hadron. In the second integral, $M_{max}^2 = Q^2(x_{I\!P}^{max}/x - 1)$ is found by demanding a large rapidity gap in the diffractive dissociation. Calculations are made both for $x_{I\!P}^{max} = 0.1$ as in [5] and for $x_{I\!P}^{max} = 0.03$ as in [8], although the former is more convenient as it guarantees the disappearance of nuclear shadowing at $x \sim 0.1$ as in experimental data. Coherence effects are taken into account in the form factor

$$F_A(t_{min}) \;=\; \int \mathrm{d}^2b\, J_0(b\sqrt{-t_{min}})\, T_A(b) \tag{5}$$

which is equal to 1 at $x \to 0$ and decreases with increasing x due to the loss of coherence for $x \geq (2m_N R_A)^{-1}$, see (2) (here we have put $t_{min} = -m_N^2 x_{I\!P}^2$).

The second order elastic cross section in (4) is obviously negative and will lead to a reduction of the total cross section. In the small x region, it is also necessary to include higher orders terms in (3) in order not to violate unitarity of the total cross section, as was noted in [9].

Summation of all terms in (3) is model dependent. The Schwimmer unitarization [10] for the total hA cross section, which also sums up all Pomeron tree diagrams, is used to obtain

$$\frac{\sigma_{\gamma^* A}^{Sch}}{A\,\sigma_{\gamma^* N}} \;=\; \int \mathrm{d}^2b\, \frac{T_A(b)}{1 \,+\, (A-1) f(x,Q^2) T_A(b)}\,, \tag{6}$$

where $f(x,Q^2)$ is the effective shadowing function. Following [11,12] in choice of parameters and factorization, one can get the shadowing function as

$$f(x,Q^2) \;=\; 4\pi \int_x^{x_{I\!P}^{max}} \mathrm{d}x_{I\!P}\; B(x_{I\!P})\, \frac{F_{2\mathcal{D}}^{(3)}(x_{I\!P},Q^2,\beta)}{F_2(x,Q^2)} \times F_A^2(t_{min})\,. \tag{7}$$

Here $B(x_{I\!P}) = 0.184 - 0.02\ln(x_{I\!P})\ \mathrm{fm}^2$. The lhs. in (6) is defined as the shadowing ratio $R^{Sch}\,(A/N)\,(x)$.

The structure function F_2 and the diffractive structure function $F_{2\mathcal{D}}$ of the single nucleon are taken as input from experiment. The extension to the nuclear case is therefore parameter-free except for the unitarity constraints leading to eq. (6). This is a remarkable feature of the Glauber-Gribov model [13].

The model is valid for low values of $x \leq 0.01$ and intermediate $Q^2 < 10\ \mathrm{GeV}^2$. In what follows, we will neglect the Q^2 dependence of the model, knowing that the presence of a strong Q^2-dependent term is not required to describe nuclear data at low Q^2 which is relevant for our present considerations [5].

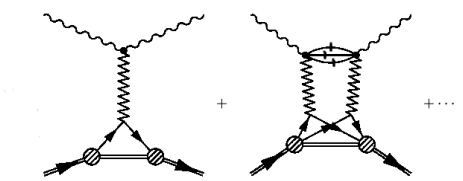

Fig. 1. The single and double scattering from to the total cross section (the diffractive intermediate states are on mass shell).

3 Inclusive and diffractive data

In deep inelastic scattering (DIS) the structure function of a nucleon is related to the total cross section of $\gamma^* N$ interaction through factorization at high scales valid in perturbative QCD. The structure function holds information about the partonic content of the nucleon, and is given by a sum of parton distribution functions (PDFs)

$$F_2\left(x,Q^2\right) \;\propto \sum_{i=g,u,d,s\dots} x f_i\left(x,Q^2\right)\,, \tag{8}$$

where the sum is over all types of partons. Similar to the inclusive DIS case, a factorization theorem has been

proved in perturbative QCD to hold for diffractive structure functions [14]. The diffractive structure function $F_{2\mathcal{D}}^{(3)}$ in eq. (7) is given by

$$F_{2\mathcal{D}}^{(3)}\left(x_{I\!P}, Q^2, \beta\right) \;=\; \overline{f}_{I\!P}\left(x_{I\!P}\right) F_2^{I\!P}\left(\beta, Q^2\right) \;, \qquad (9)$$

where $\overline{f}_{I\!P}$ is the t-integrated Pomeron flux and we have assumed so-called Regge factorization. The Pomeron flux factor is defined as

$$\overline{f}_{I\!P}\left(x_{I\!P}\right) \;=\; \int_{t_{cut}}^{t_{min}} \frac{e^{B_0\, t}}{x_{I\!P}^{2\alpha_{I\!P}(t)-1}}\, \mathrm{d}t \;, \qquad (10)$$

where we assume a linear Pomeron trajectory, $\alpha_{I\!P}(t) = \alpha_{I\!P}(0) + \alpha'_{I\!P} t$. The values of the parameters are taken to be $\alpha_{I\!P}(0) = 1.173$ and $\alpha'_{I\!P} = 0.26$ GeV^{-2}, and we put $B_0 = 4.6$ GeV^{-2} (see [15] for details). $F_2^{I\!P}$ is called the structure function of the Pomeron, and so it is possible to introduce a partonic structure of the Pomeron [16], as in eq. (8).

For both inclusive and diffractive DIS, the gluon content clearly dominates over the quark one at low x and intermediate Q^2 values relevant to our present considerations. In what follows we will only consider the gluon parton distribution functions of the nucleon and Pomeron. Quark shadowing was discussed in [5]. The ratio under the integral in eq. (7) can, in other words be understood as the density of gluons in the Pomeron compared to the density of gluons in the nucleon!

For the nucleon structure function we will use the next to leading order (NLO) ZEUS-S QCD fit of the gluon PDF [17] at $Q^2 = 7$ GeV^2. The gluon diffractive parton distribution function (dPDF) was measured for intermediate Q^2 at both HERA experiments: ZEUS and H1. The situation regarding the gluon content of the Pomeron is at present rather uncertain with a large discrepancy between the presented results. The origin of the discrepancy is unknown. We will make calculations for three different fits which we will briefly mention

- H1 NLO QCD 2002 fit [12] (large-rapidity-gap data, gives also a good description of heavy quark and dijet production)
- H1 & ZEUS 2005 fit [18] (H1 NLO QCD analysis of ZEUS M_X-data)
- H1 NLO QCD 2006 fit [19,20] (forward proton spectrometer data, fit A was used)

The gluon dPDF for the Pomeron was parameterized at fixed $Q^2 = 6.5$ GeV^2 ($Q^2 = 8.5$ GeV^2 in the second case). Both inclusive and diffractive distributions were fitted by a simple function

$$x\, f_g\left(x, Q^2\right) \;=\; x\, f_g\left(x\right) \;=\; A x^{-\delta}\left(1-x\right)^{\gamma} \;, \qquad (11)$$

where A, δ and γ are fitting parameters.

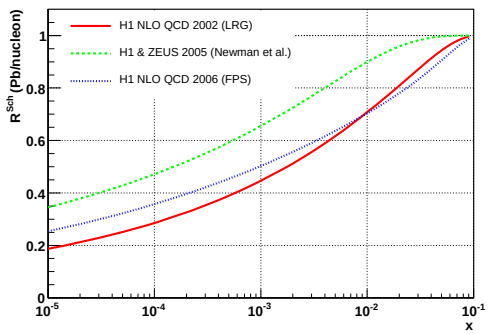

Fig. 2. Nuclear shadowing ratio R(Pb/N) for different parameterizations of the diffractive gluon parton distribution function.

4 Nuclear shadowing ratio

Numerical calculations of the nuclear shadowing ratio for Pb, defined in eq. (6), for different parameterizations of the gluon dPDF as described in the previous section are presented in Fig. 2. The fit to ZEUS data [18] predicts weakest gluon shadowing, while the fits to the both of the H1 datasets are compatible with each other and predict a much stronger shadowing effect. The strongest gluon shadowing is obtained for the H1 NLO QCD 2002 fit [12], which is almost twice as big as the ZEUS one [18] for the whole range of x.

Gluon shadowing for various heavy ions (Ca, Pd and Pb) calculated with (6) is presented in Fig. 3 (H1 NLO QCD 2002 fit [12] is used). The effect is strong at small x, and disappearing at $x = x_{I\!P}^{max}$. This is a consequence of the coherence length in the form factor (5), and the vanishing integration domain in (7). Gluon shadowing is as low as 0.2 for the Pb/N ratio at $x \sim 10^{-5}$.

A comparison of our results for Pb/nucleon ratio at $Q^2 = 6.5$ GeV^2 with $x_{I\!P}^{max} = 0.03$, with other models, calculated at $Q^2 = 5$ GeV^2, is presented in Fig. 4 (H1 NLO QCD 2002 fit [12] is used). In [21], the authors have calculated shadowing within the BFKL formalism [22], while [23] is based on a parameterization of pp-data. The authors of [8] make their calculations within a similar framework as the presented model.

For $x \leq 10^{-3}$ our model predicts stronger gluon shadowing compared to [21] (dashed-dotted line) and [8] (dotted line), while [23] (dashed line) predicts the strongest effect down to $x \sim 10^{-4}$. Our calculations are close to the predictions of [8] for $x > 10^{-3}$ for this choice of $x_{I\!P}^{max}$, while we are consequently below the predictions of [21].

5 Shadowing effects in d+Au collisions

The model is now employed to study particle production in d+Au collisions at RHIC energy $\sqrt{s} = 200$ GeV. There has been observed an increasing suppression of the nuclear modification factor (NMF)

$$R_{dAu} \;=\; \frac{1}{\langle N_{coll}\rangle}\, \frac{\mathrm{d}^2 N^{dAu} / \mathrm{d}p_T \mathrm{d}\eta}{\mathrm{d}^2 N_{inel}^{pp} / \mathrm{d}p_T \mathrm{d}\eta} \qquad (12)$$

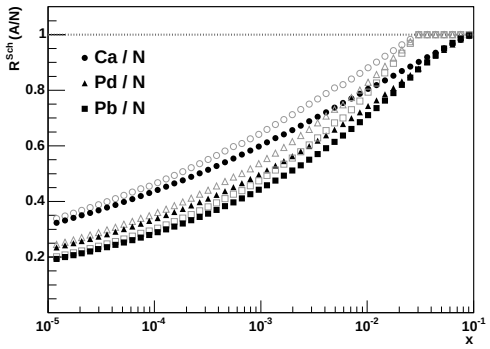

Fig. 3. Gluon shadowing for heavy ions. Closed (open) symbols are for $x_{I\!P}^{max} = 0.1$ (0.03).

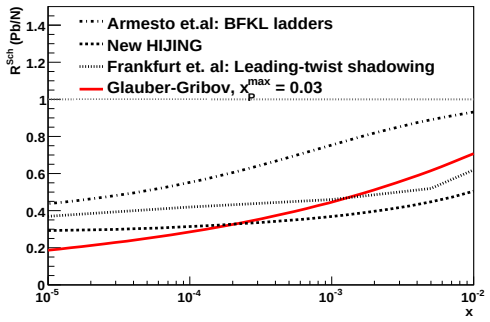

Fig. 4. Comparison of our results the Pb/nucleon ratio with other models, at fixed Q^2.

with increasing pseudorapidity of the observed particle [24]. Various models have been utilized to explain the observed features, the most successful of which is the Color-Glass-Condensate (CGC) model [25], which assumes gluon saturation for the kinematical domain reached in hadron-nucleus collisions at RHIC. It is instructive to point out, that the model presented here does not assume a saturation scale, like in [25]. Yet, as we have already mentioned, Pomeron interactions are taken into account to preserve unitarity of the scattering amplitude. In this sense it should give similar results as models assuming gluon ladder fusion.

In the Glauber-Gribov model, the multiplicity reduction due to shadowing compared to the simple Glauber model is easily obtained in a factorized form. The theoretical prediction is given by [26]

$$R_{dAu}^{theo} \;=\; R_d^{Sch}(x_p) R_{Au}^{Sch}(x_t)\,, \qquad (13)$$

where the deuteron will be treated as a point particle in impact parameter space, but with the shadowing found from (6). The collision is described by the following jet kinematics

$$x_{p(t)} \;=\; c\, p_T\, e^{\pm\eta}/\sqrt{s}\,, \qquad (14)$$

for the projectile (target) x-value respectively. In eq. (14) p_T is the transverse momentum of the particle, and we assume that most of the high-p_T particles come from jets c times more energetic.

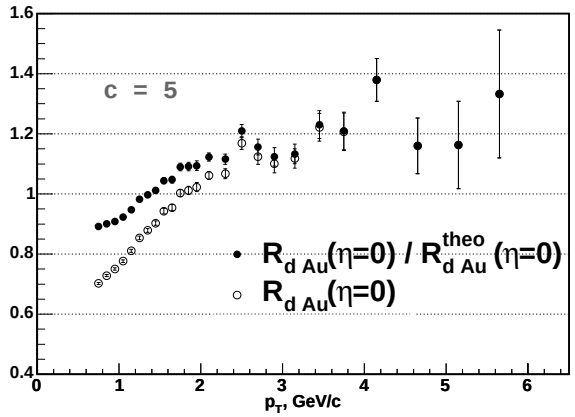

Fig. 5. Shadowing effects for d+Au collisions $\sqrt{s} = 200$ GeV at midrapidity for $c = 5$.

An important and well-known effect that is not taken into account in the model presented here, is the Cronin effect [27,28], or p_T-broadening of the produced particles, which leads to an effective enhancement of the NMF seen at midrapidity for $p_T > 2$ GeV [24,29]. In what follows we will assume that this effect stays the same for all pseudorapidities.

We therefore extract the gluon shadowing effects in the NMF at $\eta = 0$ by defining $R_{dAu}^{norm} = \left[R_{dAu}^{exp}/R_{dAu}^{theo}\right]_{\eta=0}$, shown in Fig. 5 for $c = 5$. As expected, the shadowing dies out at high p_T.

The multiplicity reduction merely due to shadowing will then appear as we compare the NMF at forward rapidities, $\eta = 1$, 2.2, 3.2 to R_{dAu}^{norm}. This can be quantified by the double ratio

$$\tilde{R} \;=\; \frac{[R_{dAu}]_\eta}{R_{dAu}^{norm}}\,, \qquad (15)$$

where the NMF in the numerator is taken at a constant rapidity slice.

The double ratio, as defined in (15), for the NMF taken from [24] is plotted together with the predictions of the Glauber-Gribov model from eq. (13) in figs. 6 and 7 for two different values of the parameter c. Calculations are made for the three gluon dPDF parameterizations described in Section 3. Statistical errors are denoted by the thick solid line, while the systematic and statistical errors added up quadratically are denoted by the dashed line. The choice of c does not seem to affect the result.

There is good agreement with experimental data for all the gluon dPDF parameterizations. The H1 NLO QCD 2002 fit seems to be most consistent with the data, and the agreement is better at higher values of pseudorapidity. Although the ZEUS fit (H1 & ZEUS 2005) is almost a factor of two smaller for the whole range of possible x, the agreement is surprisingly good. This gives evidence for a dominating shadowing contribution to the suppression of the NMF at forward rapidities at RHIC energies.

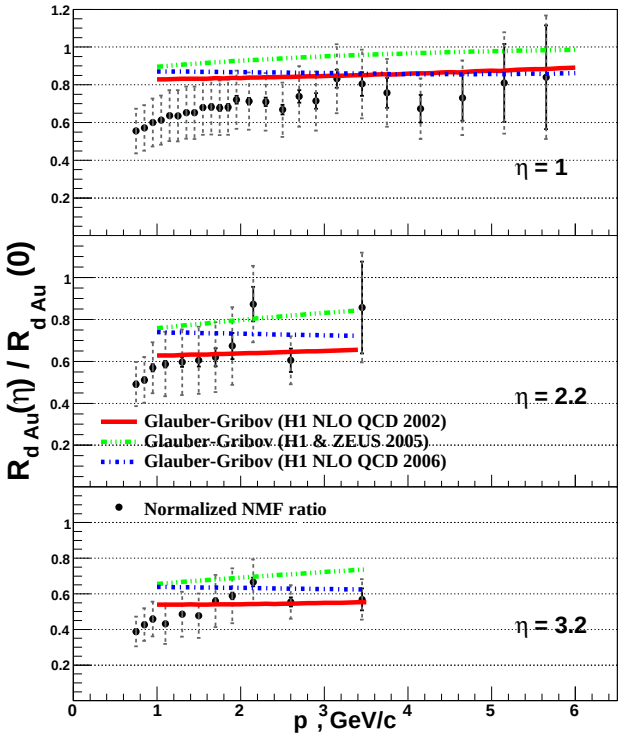

Fig. 6. NMF ratio, $c = 3$

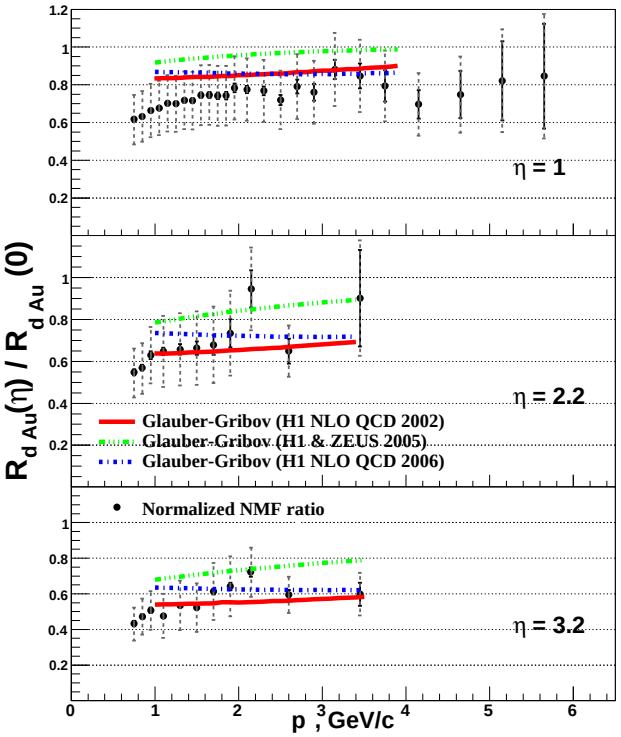

Fig. 7. NMF ratio, $c = 5$

6 Nuclear shadowing at SPS

We have also calculated the nuclear shadowing ratio for lower energies, namely at maximal SPS energy $\sqrt{s} = 17.3$ GeV. In Fig. 8 we show the calculation of the Glauber-Gribov model compared to data on charged pion production for fixed $x_F = 0.375$ taken from [30] for the double ratio defined in eq. (15) (the H1 NLO QCD 2002 fit was used). The curves are for two values of the parameter c, and we see that the shadowing disappears quickly with increasing c.

Obviously, the effect of gluon shadowing is not sufficient to explain the observed suppression at this energy. The solid curve in Fig. 8 can be taken as the maximum value of the effect. The suppression in the experimental data is strongest for small p_T.

Theoretical considerations on the reasons for the suppression in the NMF at SPS energies are out of the scope of the present paper, but will be followed up in the nearest future [32]. An extremely interesting fact is that the suppression at SPS is almost of the same magnitude as at RHIC energies. Since gluon shadowing is expected to become significant with growing energy of the reaction, there is apparently another mechanism present which is responsible for the suppression. This mechanism is related to the energy-scale relevant for coherent scattering; at these energies a large fraction of the Fock-state of the incoming hadron will rescatter as in the Glauber model [31]. Energy-momentum conservation effects, which violate the AGK cutting rules, will play a dominant role [33].

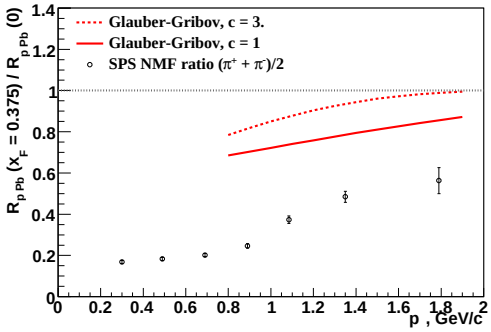

Fig. 8. Shadowing ratio for $\sqrt{s} = 17.3$GeV in the fragmentation region.

7 Conclusions

We have presented results for the nuclear shadowing ratio, eq. (6), and particle production in hadron-nucleus collisions for various parameterizations of the gluon dPDF within the Glauber-Gribov model, and compared them to experimental data on the nuclear modification factor measured at two different energies, $\sqrt{s} = 17.3$ GeV and $\sqrt{s} = 200$ GeV. Our calculations of the nuclear shadowing ratio is consistent with other models predicting large gluon shadowing for low values of x and intermediate Q^2.

For RHIC energies, the suppression of the NMF observed at non-zero values of pseudorapidity is well described by gluon shadowing within the Glauber-Gribov model. The experimental data on gluon dPDF is still quite

uncertain, and introduces a large spread in the theoretical prediction. The agreement with experimental data is reasonable for all the presented parameterizations.

We would like to underline that the results we have presented can be viewed as an upper bound of the effect of gluon shadowing in hadron-nucleus collisions. The authors of [34] have done calculations within a similar framework with a different choice of kinematics than in eq. (14), resulting in a much weaker shadowing effect. This discrepancy is important to resolve in the nearest future.

In [34] there is also an important remark on the experimental data from BRAHMS [24] at the two most forward rapidities. The fact that only negative particles, h^-, are measured leads effectively to an enhancement of the NMF because of isospin effects. In order to compare to the correct NMF, one should reduce the experimental data at $\eta = 2.2$ and 3.2 by a factor of $\sim 2/3$. This will lead to a less impressive agreement of our model, yet it will not change the conclusions regarding gluon shadowing at RHIC.

At SPS, the gluon shadowing is not responsible for more than 10 % of the total suppression. The important fact, however, is the observed large suppression up to $p_T =$ 2 GeV/c at such low energies. The suppression seems in fact to be approximately of the same magnitude as at RHIC, where $\sqrt{s}$ is a factor of ten larger. The suppression is caused by energy-momentum conservation which should stay constant with growing energy. This may indicate that our estimates of gluon shadowing are too large.

The energy-dependence of the suppression is related to the underlying space-time dynamics of the collision, and is therefore a crucial test for theoretical models. With new low-energy data on NMF in the forward region a comparison of the effect can now also be done for $x_F > 0$. This gives an opportunity to study the interplay of different effects leading to suppression/enhancement of particle spectra in much more detail.

The presented model can also be used to calculate the expected suppression in heavy-ion collisions at LHC energies [32].

K. T. would like to thank for warm hospitality at SINP in Moscow State University and ITEP, where part of this work has been done. The authors would also like to thank B. Boimska for providing experimental data. Useful discussions with D. Röhrich, M. Strikman and L. Frankfurt are gratefully acknowledged. This work has been supported by the agreement between the Department of Physics, the University of Oslo and SINP MSU.

References

1. M. Arneodo, Phys. Rep. **240**, 301 (1994)
2. R. J. Glauber, in Lectures in Theoretical Physics, edited by W.E. Brittin and L.G. Dunham (Interscience, N.Y., 1959), Vol. 1, p. 315
3. V. N. Gribov, Sov. Phys. JETP **29**, 483 (1969); *ibid.* **30**, 709 (1970)
4. A. Kaidalov, Nucl. Phys. A **525**, 39c-58c (1991)
5. A. Capella, et al., Eur. Phys. J. C **5**, 111 (1998); N. Armesto, et al., Eur. Phys. J. C **29**, 531 (2003)
6. V.A. Abramovsky, V.N. Gribov, O.V. Kancheli, Sov. J. Nucl. Phys. **18**, 308 (1974)
7. V. N. Gribov, Sov. Phys. JETP **26**, 414 (1968)
8. L. Frankfurt, V. Guzey and M. Strikman, Phys. Rev. D **71** 054001 (2005)
9. A. B. Kaidalov, V. A. Khoze, A. D. Martin, M. G. Ryskin, Phys. Lett. B **567**, 61 (2003)
10. A. Schwimmer, Nucl. Phys. B **94**, 445 (1975)
11. A. Capella, et al., Phys. Rev. D **63**, 054010 (2001)
12. C. Adloff et al. [H1 Collaboration], Z. Phys. C **76**, 613 (1997); H1 Collaboration, paper **980** submitted to ICHEP 2002, Amsterdam (2002)
13. N. Armesto, `hep-ph/0604108`
14. J. C. Collins, Phys. Rev. D **57**, 2051 (1998). Erratum, *ibid.* D **61** 019902 (2001)
15. V. Barone, E. Predazzi, *High-Energy Particle Diffraction*, Springer-Verlag Berlin Heidelberg (2002)
16. G. Ingelman, P. E. Schlein, Phys. Lett. B **152**, 256 (1985)
17. S. Chekanov et al. [ZEUS Collaboration], Phys. Rev. D **67**, 012007 (2003)
18. P. Laycock, P. Newman, F. P. Schilling, AIP Conf. Proc. 729, 466 (2005)
19. H1 Collaboration, `hep-ex/0606003`, DESY-06-048
20. H1 Collaboration, `hep-ex/0606004`, DESY-06-049
21. N. Armesto, Eur. Phys. J. C **26**, 35 (2002)
22. L. N. Lipatov, Sov. J. Nucl. Phys. **23**, 338 (1976) E. A. Kuraev, L. N. Lipatov, V. S. Fadin, Sov. Phys JETP **45**, 199 (1977) Y. Y. Balitsky, L. N. Lipatov, Sov. J. Nucl. Phys. **28**, 822 (1978)
23. S.Y. Li and X.N. Wang, Phys. Lett. B **527**, 85 (2002)
24. I. Arsene, et al. [BRAHMS Collaboration], Phys. Rev. Lett. **93**, 242303 (2004)
25. D. Kharzeev, Y. V. Kovchegov, K. Tuchin, Phys. Rev. D **68**, 094013 (2003)
26. A. Capella, A. Kaidalov, J. Tran Thanh Van, Heavy Ion Phys. **9**, 169 (1999)
27. J. W. Cronin et al., Phys. Rev. D **11**, 3105 (1975)
28. D. Antreasyan et al., Phys. Rev. D **19**, 764 (1979)
29. H. Buesching [PHENIX Collaboration], nucl-ex/0410002
30. B. Boimska, Ph. D. Dissertation (Warsaw 2004), CERN-THESIS-2004-035
31. B. Z. Kopeliovich, J. Nemchik, A. Schafer, A. V. Tarasov, Phys. Rev. Lett. **88**, 232303 (2002)
32. I. C. Aresene, L. Bravina, A. B. Kaidalov, K. Tywoniuk, E. Zabrodin, to be published elsewhere.
33. K. Boreskov, A. Capella, A. Kaidalov, J. Tran Thanh Van, Phys. Rev. D **47**, 919 (1993)
34. V. Guzey, M. Strikman, W. Vogelsang, Phys. Lett. **B** 603, 173 (2004)